Effects of the Matrix of a Macronet Sulfonated Polystyrenic Resin on H^+/Mg^{2+} and H^+/Ca^{2+} Ion Exchange Kinetics

SORINELA DANIELA CANTEA[1]*, EUGEN PINCOVSCHI[1], ANA-MARIA S. OANCEA[2]

[1]University Politehnica of Bucharest, Department of Analytical Chemistry and Environmental Engineering, 1-3 Gh. Polizu Str., 011061 Bucharest, Romania

[2]University Politehnica of Bucharest, Department of Inorganic Chemistry, Physical Chemistry and Electrochemistry, 1-3 Gh. Polizu Str., 011061 Bucharest, Romania

A new polymeric resin with styrene-divinylbenzene hyper-reticulated matrix and sulfonic functional groups designated as a macronet resin was evaluated from the kinetic point of view for magnesium and calcium ions removal by ion exchange in the demineralization process. The ion exchanger contains macro-, meso- and micropores. The ion exchange rate was measured at 298 K with a potetiometric method in conditions favouring a particle diffusion controlled mechanism. The results were modeled using both quasi-homogeneous resin phase and bidisperese pore kinetic models. The H^+/Mg^{2+} and H^+/Ca^{2+} integral interdiffusion coefficients were computed and compared. It was shown that the matrix of the macronet resin produced a retarding effect on ion diffusion compared to dilute aqueous solution of about two orders of magnitude. The bidisperese pore kinetic model allowed the evaluation of the upper limit of the ratio between the ion exchange capacity due to the sulfonic groups bound on micropores and macropores walls, for three hypotheses: a) the ion interdiffusion takes place step-by-step in macropores and micropores; b) the ion interdiffusion in macro- and micropores is competitive, but ten times faster in macropores; c) the ions diffuse in parallel in macro- and micropores with the same rate. The plausible ratio between the micropores an macropores uptake at equilibrium of the macronet resin for H^+/Mg^{2+} and H^+/Ca^{2+} ion exchange was evaluated as 1/30, 2/1 and 10/1 in cases a), b) and c), respectively.

Keywords: ion exchange kinetics; magnesium ion; calcium ion; macronet resin; hypercrosslinked polymer; polystyrenic resin; interdiffusion coefficient; porous ion exchangers

The most important industrial application of the ion exchange procedure is demineralization, which implies removal also of magnesium and calcium ions. The properties of the ion exchanger are crucial for an efficient and economic demineralization process. A third generation of styrene-divinylbenzene sulfonated ion exchanger with macro-, meso-, and micropores is now available as commercial product [1], but it was scarcely investigated in the open literature. Few papers investigating ion exchange equilibria [2-6] and kinetics [7, 8] on the strong acid macronet resin Purolite MN500 were reported. No data for magnesium and calcium ion exchange kinetics on this material were published to our knowledge. This class of polymers was developed by Davankov and Tsyurupa [9, 10]. The hyper-reticulation was introduced in the styrene-divinylbenzene copolymer by post-crosslinking the swelled polymers in a solvent in large excess with conformational rigid bridges [9, 10]. The macronet Purolite MN500 strong acid cation exchanger has a cauliflower structure, a spherical bead being formed by clusters of spherical gel microparticles containing micropores, and between the aggregated microparticles there are meso- and macropores [11]. The inert polymers have a high surface area of 1000 $m^2 g^{-1}$, and after sulfonation the surface area decreased to around 300 $m^2 g^{-1}$ [11].

The main objective of the present work was to investigate H^+/Mg^{2+} and H^+/Ca^{2+} ion exchange kinetics on the strong acid macronet ion exchanger Purolite MN500 in order to evaluate this material for demineralization process. The specific objectives were: a) experimental determination of the ion exchange rate in conditions favouring a mechanism controlled by particle diffusion; b) modeling of the kinetic curves with quasi-homogeneous resin phase models and with a bidisperse pore model; c) comparison and discussion of the interdiffusion coefficients obtained with different kinetic models; d) evaluation of H^+, Mg^{2+} and Ca^{2+} self-diffusion coefficients in the strong acid macronet resin.

Quasi-homogeneous resin phase kinetic models

Ion exchange kinetics is mainly a diffusional process and was described as an isotopic exchange, using the Fick's equations for the flux and material balance. Two limiting mechanisms were considered: a) the controlling step of the ion exchange kinetics is the ion interdiffusion in the Nernst fictitious film surrounding the spherical particle of the ion exchanger (film diffusion control); b) the interdiffusion of ions inside the bead of the ion exchanger is the rate controlling step (particle diffusion control). This treatment implies the assumption that the resin phase is quasi-homogeneous (QHRP), the diffusion coefficient is an effective diffusivity and it is a constant, and the neglecting of the contribution of the electrical forces to ion interdiffusion. The objective of the present work was to evaluate the ion interdiffusion inside the macronet particle, thus the kinetic equations for particle diffusion controlled mechanism will be presented. The Fick second equation for particle diffusion control and spherical particles was integrated at infinite solution volume boundary condition (ISV) and the fractional attainment of equilibrium is given by equation 1 (F-ISV) [12]:

* *email: cadana2003@yahoo.com; Tel.: 0755793940*

Table 1

THE CORRESPONDENCE BETWEEN β / α PARAMETER AND $M_{i\infty}/M_{a\infty}$ RATIO

β/α	0.003	0.01	0.03	0.05	0.075	0.1	0.3	1	3	6	30	300
$M_{i\infty}/M_{a\infty}$	1/1000	1/300	1/100	1/60	1/40	1/30	1/10	1/3	1/1	2/1	10/1	100/1

$$F(t) = 1 - \frac{6}{\pi^2}\sum_{n=1}^{\infty}\frac{1}{n^2}\exp\left(-n^2\pi^2\tau\right) \qquad (1)$$

The half-time of the process derived from equation 1 is [12]:

$$t_{1/2} = 0.030\frac{\bar{r}_0^2}{\bar{D}} \qquad (2)$$

Reichenberg proposed a simplified equation valid for $F < 0.85$ [13], which is an approximation of equation 1 at ISV, but avoiding the problems related to the series convergence:

$$F(t) = \frac{6}{\pi^{3/2}}\left(\pi^2\tau\right)^{1/2} - \frac{3}{\pi^2}\left(\pi^2\tau\right) \qquad (3)$$

The usual kinetic measurements are done in batch reactors, thus the finite solution volume boundary condition (FSV) is the rigorous one. The analytical solution of the Fick's second law at FSV (F-FSV) is [12]:

$$F(t) = 1 - \frac{2}{3\omega}\sum_{n=1}^{\infty}\frac{\exp\left(-S_n^2\tau\right)}{1 + S_n^2/9\omega(\omega+1)} \qquad (4)$$

where S_n are the roots of equation $S_n \cot S_n = 1 + S_n^2/3\omega$.

Paterson developed an approximation for FSV for $\tau < 0.1$ eluding the series convergence problem [12]:

$$F(t) = \frac{\omega+1}{\omega}\left(1 - \frac{1}{\alpha'-\beta'}\left[\alpha'\exp\left(\alpha'^2\tau\right)\left(1+erf\alpha'\tau^{1/2}\right) - \right.\right.$$
$$\left.\left. - \beta'\exp\left(\beta'^2\tau\right)\left(1+erf\beta'\tau^{1/2}\right)\right]\right) \qquad (5)$$

where α' and β' are the roots of the equation $x^2 + 3\omega x - 3\omega = 0$.

Bidisperse pore kinetic model

The QHRP hypothesis for a porous ion exchanger is a drastic approximation and this is the reason that a bidisperse pore kinetic model was also taken into account. The model was developed for sorption of species from fluid media in a porous solid with macro- and micropores, at ISV with constant diffusion coefficient in macro- and micropores [14].

The fractional attainment of equilibrium vs. time for competitive diffusion in macropores and micropores (BDM-CD) was given [14] as:

$$F = \frac{M_t}{M_\infty} = \frac{\sum_{k=1}^{\infty}\sum_{q=1}^{\infty}\frac{k^2\left[1-\exp\left(-\alpha\xi_{qk}^2\theta\right)\right]}{\xi_{qk}^4\left[\frac{\alpha}{\beta}+1+\cot^2\xi_{qk}-\left(1-\frac{k^2\pi^2}{\beta}\right)\frac{1}{\xi_{qk}^2}\right]}}{\sum_{k=1}^{\infty}\sum_{q=1}^{\infty}\frac{k^2}{\xi_{qk}^4\left[\frac{\alpha}{\beta}+1+\cot^2\xi_{qk}-\left(1-\frac{k^2\pi^2}{\beta}\right)\frac{1}{\xi_{qk}^2}\right]}} \qquad (6)$$

where ξ_{qk} are the roots of transcendental equation:

$$\beta\left(1-\xi_{qk}\cot\xi_{qk}\right)+\alpha\xi_{qk}^2 = k^2\pi^2;\ \ k = 1,2,3,\cdots\infty$$

The equation describing a limiting case (BDM-LC) in which the ion exchange process is assumed as *a step-by-step diffusion in macro- and micropores* (the diffusion is 10^3 times faster in macropores than in micropores) was given [14] as:

$$F = \frac{M_t}{M_\infty} =$$
$$= \frac{\left[1-\frac{6}{\pi^2}\sum_{n=1}^{\infty}\frac{1}{n^2}\exp\left(-n^2\pi^2\theta\right)\right]+\frac{1}{3}(\beta/\alpha)\left[1-\frac{6}{\pi^2}\sum_{n=1}^{\infty}\frac{1}{n^2}\exp\left(-n^2\pi^2\alpha\theta\right)\right]}{1+\frac{1}{3}(\beta/\alpha)} \qquad (7)$$

The parameter $\alpha = \bar{D}_i\bar{r}_0^2/\bar{D}_a\bar{r}_i^2$ has the physical meanings of the relative rates of uptake by micropores and macropores, and $\beta/\alpha = 3M_{i\infty}/M_{a\infty}$ is three times the ratio of micropores and macropores uptakes at equilibrium, respectively. The correspondence between the parameter β/α and $M_{i\infty}/M_{a\infty}$ is given in table 1.

Interdiffusion coefficients

The presented QHRP and BDM kinetic models assume isotopic exchange and constant diffusion coefficient. The interdiffusion coefficients for mutual ion exchange processes vary with the ionic composition of the resin [12]. Calculated with these models (eq. 1-7) the interdiffusion coefficients are different constants, one for each 0-F interval, *called integral interdiffusion coefficients* [15].

Experimental part

Materials and methods

The commercial Purolite MN500 macronet strong acid resin was air dried, sieved in size fractions and purified in three cycles of successive treatments with 1M HCl solution, demineralized water with specific conductivity of 0.055 μS/cm, 1M NaOH solution, demineralizated water. The final form of the resin was H^+, and the final washing was done with demineralizated water until the effluent had a specific conductivity less than 1μS/cm. After purification the resin was air–dried and kept in a desiccator on saturated NaCl solution in order to reach a constant mass at room temperature. The properties of the studied resin are given in table 2.

The external solutions were prepared from $Mg(NO_3)_2 \cdot 6H_2O$ and $Ca(NO_3)_2 \cdot 4H_2O$ p.a. Merck, using demineralized water (~0.055 μS/cm). HCl 36% and NaOH p.a. Merck were used for the preparation of the other solutions.

Determination of the ion exchange kinetic curves

The ion exchange rate was measured in a batch reactor at 298 K with a potentiometric method monitoring the pH in the external solution during H^+/Mg^{2+} or H^+/Ca^{2+} ion exchange on the macronet resin with WTW inoLab *p*H/cond 740 meter. The accuracy was ±0.001 *p*H units. The procedure was previously described in detail [7-8, 16-17]. The ion exchange rate was measured in conditions favouring a particle diffusion control, namely in concentrated external solutions (0.93 eq/L $Mg(NO_3)_2$ and 0.95 eq/L $Ca(NO_3)_2$ under efficient stirring (500 and 600 min^{-1}). Blanc experiments shown that the electrolyte desorption during the kinetic run was negligible. The

Resin		Size fraction; sieve aperture / (μm)			
		[+300]	[+425]	[+600]	[+710]
Matrix*	Styrene-divinylbenzene; hyper-reticulated; macronet				
functional groups*	$-SO_3H$				
weight capacity (Na^+ form) / (eq/kg)**	2.52				
bulk density / (g cm^{-3})***		0.786	0.754	0.730	0.811
apparent density / (g cm^{-3})***		1.60	1.46	1.44	1.59
surface area S_{Hg} / (m^2 g^{-1})***		26	26	27	20
surface area BET, N_2 / (m^2 g^{-1})***		297	313	356	360
total cumulative pore volume / cm^3 g^{-1})***		0.65	0.64	0.68	0.60
porosity (%)***		51	48	49	49
average pore diameter / (nm)***		153	150	143	145
most frequent pore diameter / (nm)***		156	155	148	148
d50 / (nm) micropores*	1.5				
moisture (%) (H^+ form)**	57.4				

*reference [1]; **this work; ***reference [3];

Table 2
CHARACTERISTICS OF THE ION EXCHANGER PUROLITE MN500

Size fraction Sieve aperture/(μm)	H^+ form $\cdot 10^3$ (m)	Mg^{2+} form $\cdot 10^3$ (m)	Ca^{2+} form $\cdot 10^3$ (m)
[-710+630]	0.338 ± 0.020	0.387 ± 0.012	0.381 ± 0.013
[-630+500]	0.283 ± 0.010	0.304 ± 0.011	0.299 ± 0.009
[-500+400]	0.219 ± 0.009	0.245 ± 0.011	0.228 ± 0.011
[-400+300]	0.168 ± 0.009	0.203 ± 0.010	0.200 ± 0.008

Table 3
AVERAGE RADIUS OF THE SWOLLEN RESIN PARTICLES OF MN500 RESIN

average values of the swollen resin particles for different size fractions were measured microscopically in H^+, Mg^{2+}, and Ca^{2+}forms, and are given in table 3, as an average of 50 measurements. The confidence limits correspond to 99% probability and a Student distribution.

Results and discussions

The experimental curves (*pH vs. time*) were used to compute the fractional attainment of equilibrium with:

$$F = \frac{10^{-pH_t} - 10^{-pH_0}}{10^{-pH_\infty} - 10^{-pH_0}} \quad (8)$$

The initial ionic strength was high (1.395 M for $Mg(NO_3)_2$, 1.425 M for $Ca(NO_3)_2$) and varied with maximum 0.9% during H^+/Mg^{2+} and H^+/Ca^{2+} ion exchange on the sulfonated macronet resin. In these conditions the variation of the proton activity coefficient can be neglected, and equation 8 is valid also for mutual ion exchange between ions with different valences. The results are given for both investigated systems in figure 1, for different size fractions at constant stirring. A good reproducibility of the data was observed. The ion exchange rate increases with the decrease of the size of the beads of the resin. The experiments performed at two different stirring speeds, 500 and 600 min^{-1}, for the same size fraction of a system, presented in figure 2 show that the stirring regime does not influence the ion exchange rate in the selected conditions. This behaviour supports an ion exchange mechanism controlled by particle diffusion for both H^+/Mg^{2+} and H^+/Ca^{2+} ion exchange processes on the strong acid macronet resin MN500.

Several kinetic equations were fitted on the F vs. time curves of the investigated systems in order to obtain empirical kinetic equations used for interpolation. The equations obtained for the best fit, the coefficients of the best fitted equations and the parameters of the goodness of fit (r-square and $F_{statistics}$) are given in table 4 for H^+/Mg^{2+} and in table 5 for H^+/Ca^{2+} on the strong acid macronet resin. These equations were used to obtain the half-time of the ion exchange process, and *F vs. t* files ($0 < F < 1$) used for computing the interdiffusion coefficients.

Figure 3 gives the linear dependence of the half-time on the square of the radius of the swollen resin beads for both H^+/Mg^{2+} and H^+/Ca^{2+} ion exchange processes on MN500 resin, also supporting the particle diffusion controlled mechanism [12]. The integral interdiffusion coefficients at half-exchange on the macronet strong acid resin were obtained using equation 2 and the slopes from the plots in figure 3 and are: $\overline{D}_{F=0.5}^{H^+/Mg^{2+}} = 1.23 \cdot 10^{-10} m^2 s^{-1}$and $\overline{D}_{F=0.5}^{H^+/Ca^{2+}} = 1.01 \cdot 10^{-10} m^2 s^{-1}$,respectively.

The integral interdiffusion coefficients were computed with QHRP kinetic models at ISV (eq. 1, 3) and at FSV (eq. 4, 5). Four computer programs reported previously [16, 17] were used. The results are presented for both investigated systems at the same size fraction in figure 4. The models at ISV and FSV give similar results for H^+/Mg^{2+} and H^+/Ca^{2+} ion exchange on sulfonated macronet MN500 resin. This prove that the experiments done in a batch reactor for a

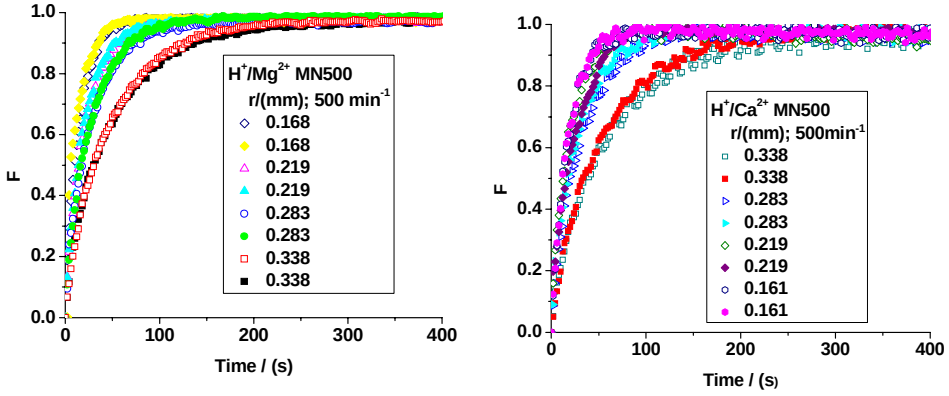

Fig. 1. Kinetic curves of H^+/Mg^{2+} and H^+/Ca^{2+} ion exchange processes on the strong acid macronet resin MN500; 298 K; 0.93 eq/L $Mg(NO_3)_2$; 0.95 eq/L $Ca(NO_3)_2$

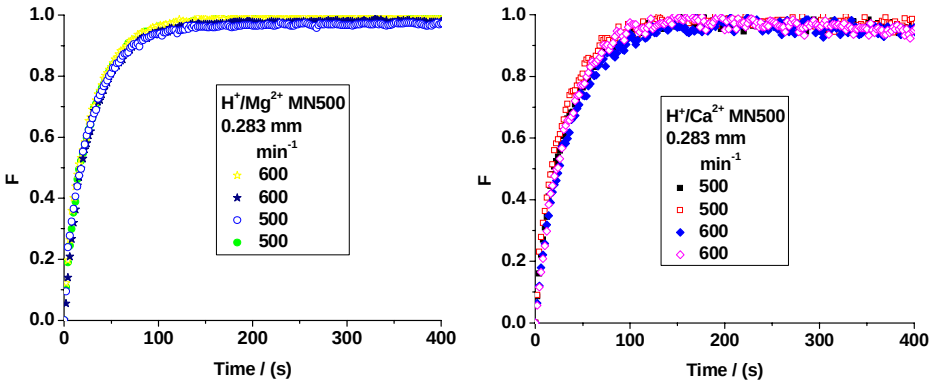

Fig. 2. Influence of the stirring speed on the ion exchange kinetics of H^+/Mg^{2+} and H^+/Ca^{2+} on MN500 resin; 298 K; 0.93 eq/L $Mg(NO_3)_2$; 0.95 eq/L $Ca(NO_3)_2$

$\bar{r}_0 10^3$ /(m)	No. exp. pcts.	*a*	*b*	*c*	*d*	r-square	F-statistics	Eq.
0.338	2432	0.591 ± 0.011	0.01840 ± 0.00028	0.397 ± 0.011	0.1500 ± 0.0088	0.9971	139749	a
0.338	1126	0.730 ± 0.013	0.01956 ± 0.00023	0.256 ± 0.014	0.273 ± 0.035	0.9988	155391	a
0.283	1420	0.756 ± 0.012	0.03385 ± 0.00038	0.236± 0.012	0.597 ± 0.072	0.9983	142312	a
0.283	2416	0.616 ± 0.016	0.03476 ± 0.00085	0.367 ± 0.016	0.266 ± 0.020	0.9931	58164	a
0.283	1828	0.768 ± 0.013	0.0355 ± 0.0006	0.222 ± 0.013	0.329 ± 0.026	0.9974	120046	a
0.283	1324	2.094 ± 0.092	0.0334 ± 0.0004	0.133 ± 0.019	0.1193 ± 0.0092	0.9984	139609	a
0.219	2358	0.713 ± 0.014	0.05053 ± 0.00095	0.278 ± 0.014	0.336 ± 0.018	0.9964	110928	a
0.219	2360	0.966 ± 0.001	0.0499 ± 0.0003	0.0297 ± 0.0020	0.0007 ± 0.0001	0.9960	98158	b
0.168	849	0.411 ± 0.070	0.213 ± 0.036	0.5742 ± 0.070	0.0554 ± 0.0042	0.9766	15091	b
0.168	2004	0.758 ± 0.016	0.0656 ± 0.0013	0.230 ± 0.016	0.91 ± 0.12	0.9946	62233	a

Table 4
COEFFICIENTS OF THE BEST FITTED EQUATION ON THE EXPERIMENTAL KINETIC CURVES FOR H^+/Mg^{2+} ION EXCHANGE ON THE STRONG ACID MACRONET RESIN MN500; 95% CONFIDENCE LIMITS; 298 K; 0.93 eq/L $Mg(NO_3)_2$

$$F = a(1-\exp(-bt)) + c(1-1/(1+cdt)) \quad \text{(a)}$$

$$F = a(1-\exp(-bt)) + c(1-\exp(-dt)) \quad \text{(b)}$$

$\bar{r}_0 10^3$ /(m)	Nr. pct. exp.	*a*	*b*	*c*	*d*	r-square	F-statistics	Eq.
0.338	2748	0.810 ± 0.040	0.0157 ± 0.0004	0.154 ± 0.040	1.2 ± 1.1	0.9654	12762	a
0.338	508	0.135 ± 0.034	0.093 ± 0.033	0.844 ± 0.033	0.0166 ± 0.0006	0.9962	22076	b
0.283	190	1.72 ± 0.24	0.0280 ± 0.0015	0.081 ± 0.053	0.108 ± 0.043	0.9971	10894	c
0.283	164	2.21 ± 0.42	0.0323 ± 0.0016	0.167 ± 0.099	0.1339 ± 0.0409	0.9969	8641	c
0.283	170	1.31 ± 0.26	0.0270 ± 0.0017	0.045 ± 0.077	0.13 ± 0.14	0.9969	9063	a
0.283	164	0.04 ± 0.20	0.09 ± 0.33	0.96 ± 0.20	0.0298 ± 0.0040	0.9972	9644	b
0.219	90	0.79 ± 0.12	0.0435 ± 0.0047	0.21 ± 0.14	2.0 ± 3.8	0.9963	3806	a
0.219	1131	0.0760 ± 0.0076	0.9815 ± 0.0006	0.0401 ± 0.0005		0.9936	49131	d
0.219	1202	0.8190 ± 0.0278	0.03633 ± 0.00100	0.1426 ± 0.0280	68.42 ± 417.50	0.9818	10758	a
0.219	634	0.1211 ± 0.0370	0.2023 ± 0.0869	0.853 ± 0.037	0.0368 ± 0.0013	0.9951	21439	b
0.168	198	0.0062 ± 0.0186	0.9774 ± 0.0038	0.0568 ± 0.0018		0.9940	8155	d
0.168	90	0.0342 ± 0.3090	0.1724 ± 1.0470	0.9532 ± 0.2985	0.0553 ± 0.0116	0.9964	3968	b

Table 5
COEFFICIENTS OF THE BEST FITTED EQUATION ON THE EXPERIMENTAL KINETIC CURVES FOR H^+/Ca^{2+} ION EXCHANGE ON THE STRONG ACID MACRONET RESIN MN500; 95% CONFIDENCE LIMITS; 298 K; 0.95 eq/L $Ca(NO_3)_2$

$$F = a(1-\exp(-bt)) + c(1-1/(1+cdt)) \quad \text{(a)}$$

$$F = a(1-\exp(-bt)) + c(1-\exp(-dt)) \quad \text{(b)}$$

$$F = a(1-\exp(-bt) - c(1+(b\exp(-nt) - n\exp(-bt))/(n-b))/n) \quad n = c+d \quad \text{(c)}$$

$$F = (a-b)\exp(-ct) + b \quad \text{(d)}$$

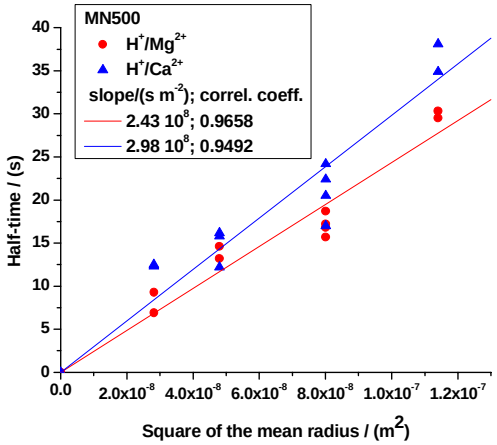

Fig. 3. Half-time *versus* square of average radius of the swollen resin particles for H^+/Mg^{2+} and H^+/Ca^{2+} ion exchange processes on the strong acid macronet resin MN500; 298 K; 0.93 eq/L $Mg(NO_3)_2$; 0.95 eq/L $Ca(NO_3)_2$

Size fraction sieve aperture / (μm)	$\bar{r}_0$ 10^3 (m)	$\bar{D}_{F=0.01}\cdot10^{10}$ ($m^2\ s^{-1}$)	$\bar{D}_{F=0.5}\cdot10^{10}$ ($m^2\ s^{-1}$)	$\bar{D}_{max}\cdot10^{10}$ ($m^2\ s^{-1}$)
		H^+/Mg^{2+}		
+630	0.338	0.0321	1.13	2.61
		0.0300	1.10	3.04
+500	0.283	0.0382	1.36	4.13
		0.0374	1.40	3.13
		0.0284	1.25	3.70
		0.0456	1.49	4.49
+425	0.219	0.0243	1.06	2.86
		0.0190	0.962	3.06
+300	0.168	0.0275	1.19	2.86
		0.0225	0.880	2.60
Average value*		0.031 ± 0.007	1.18 ± 0.17	3.25 ± 0.56
		H^+/Ca^{2+}		
+630	0.338	0.0381	0.887	2.16
		0.0252	0.969	2.86
+500	0.283	0.0322	1.16	3.60
		0.0474	1.39	4.14
		0.0237	0.982	3.12
		0.0214	1.06	4.00
+425	0.219	0.0477	1.17	3.62
		0.0222	0.874	2.52
+300	0.168	0.0343	0.669	2.30
		0.0138	0.679	2.46
Average value*		0.031 ± 0.01	0.97 ± 0.16	2.98 ± 0.55

*99% confidence limits for Student distribution

Table 6
H^+/Mg^{2+} and H^+/Ca^{2+} INTEGRAL INTERDIFFUSION COEFFICIENTS ON THE STRONG ACID MACRONET RESIN MN500 FOR DIFFERENT SIZE FRACTIONS OBTAINED WITH PATERSON $\tau < 0$ QHRP-FSV KINETIC MODEL

Ion	Crystal radius (Å)	Hydrated radius* (Å)	$\bar{D}$ *** x10^9 ($m^2\ s^{-1}$)
H^+		2.82	9.311
Mg^{2+}	0.65*	4.28	0.706
	0.86 (CN 6)**		
Ca^{2+}	0.99*	4.12	0.792
	1.14 (CN 6)**		

*[18]; **[19]; ***[20]; CN – coordination number

Table 7
IONIC RADII AND SELF-DIFFUSION COFFICIENTS IN THE DILUTE AQUEOUS SOLUTION $\bar{D}$ AT 298 K

ratio between the volume of solution and the mass of resin equal to 100 mL/g and the ratio ω (between the amount of ions in the resin phase and in solution at equilibrium) less than 0.03 are in good agreement also with ISV boundary condition. It must be noted that equations 1 and 4 are not convergent for $n = 10$ and $F < 0.1$. The Reichenberg approximation at ISV (eq. 3) and the Paterson approximation at FSV (eq. 5) give results for interdiffusion coefficients in very good agreement with the rigorous equations 1 and 4, respectively, and allowed calculations when the series (eq. 1 and 4) are not convergent.

The integral interdiffusion coefficients obtained with Paterson's model for different size fractions of the resin for H^+/Mg^{2+} and H^+/Ca^{2+} are given in table 6, for $F = 0.001$ and 0.5, together with their maximum values. The interdiffusion coefficients depend also on the size fraction, behaviour due to the differences in the crosslinking degree for resin particles with different size. During synthesis the divinylbenzene monomer reacts faster than styrene [12]. The small particles are more crosslinked than the larger particles, which are formed by growing of the small particles. The interdiffusion coefficients decrease for the smallest size fraction, in accordance with a higher crosslinking degree expected for these small particles. The Helfferich minority rule [12] allowed the evaluation of the self-diffusion coefficients in the macronet resin. This rule states that the interdiffusion coefficients in the ion exchanger tend to the self-diffusion coefficients in the ion exchanger of the ion in trace concentration [12]. Thus, $\bar{D}^{H^+/Mg^{2+}}_{F=0.01} \rightarrow \bar{D}^{Mg^{2+}}$ and $\bar{D}^{H^+/Ca^{2+}}_{F=0.01} \rightarrow \bar{D}^{Ca^{2+}}$ and $\bar{D}_{max} \rightarrow \bar{D}^{H+}$. The average values of $\bar{D}_{F=0.01}$ and of $\bar{D}_{max}$ tend to the self-diffusion coefficients of Mg^{2+}, Ca^{2+}, and H^+ on macronet MN500 resin, respectively and show a retarding and leveling effect of the resin matrix compared with the self-diffusion coefficients of the ions in dilute aqueous solution, given in

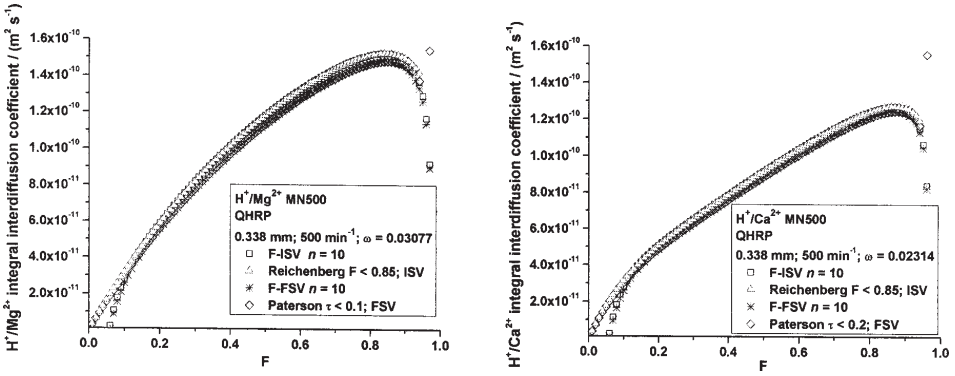

Fig. 4. The comparison of QHRP kinetic models used for computation of H^+/Mg^{2+} and H^+/Ca^{2+} integral interdiffusion coefficients on macronet MN500 resin; 298 K; 0.93 eq/L $Mg(NO_3)2$; 0.95 eq/L $Ca(NO_3)_2$

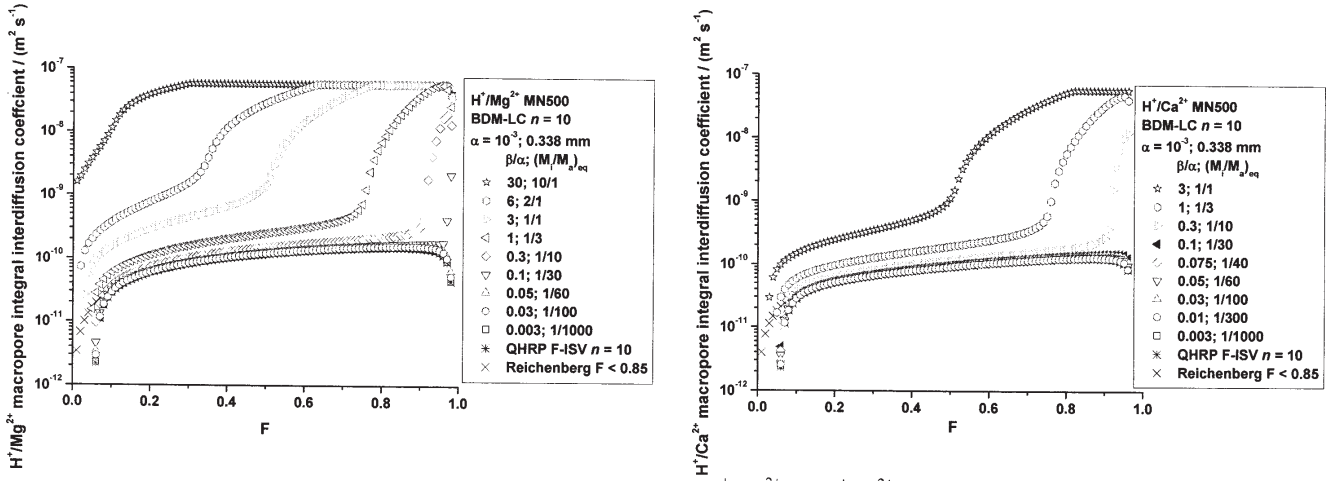

Fig. 5. H^+/Mg^{2+} and H^+/Ca^{2+} macropore integral interdiffusion coefficients on macronet MN500 resin obtained with BDM-LC kinetic model; 298 K; 0.93 eq/L $Mg(NO_3)_2$; 0.95 eq/L $Ca(NO_3)_2$

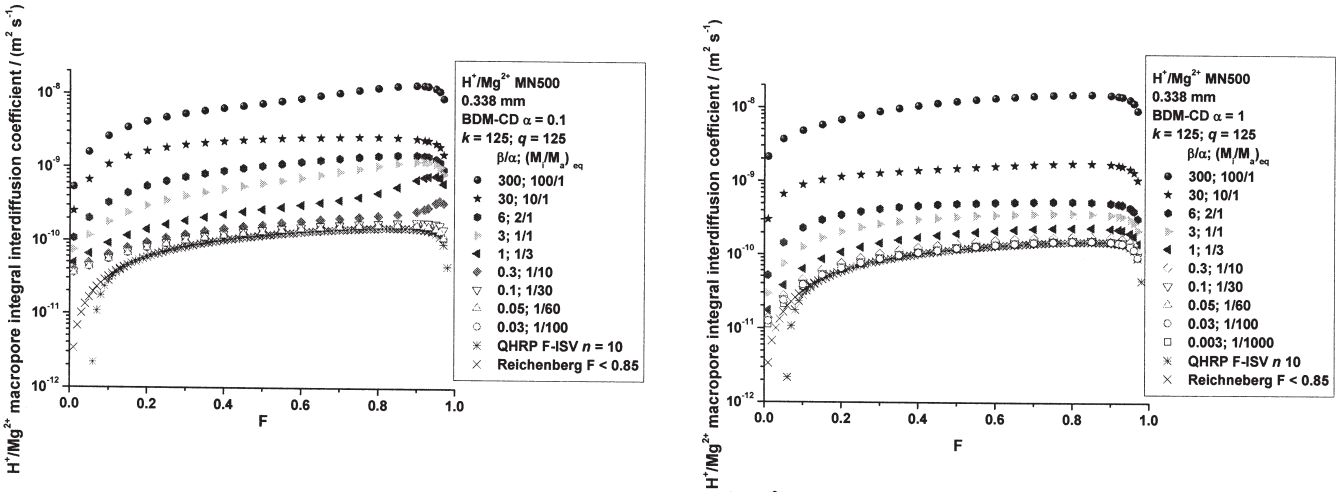

Fig. 6. H^+/Mg^{2+} macropore integral interdiffusion coefficients on macronet MN500 resin obtained with BDM-CD kinetic model; 298 K; 0.93 eq/L $Mg(NO_3)_2$

table 7. In dilute aqueous solution Ca^{2+} ion diffuses faster than Mg^{2+} ion, in accordance with their hydrated ionic radius (table 7). The leveling effect of the resin matrix supports the hypothesis that calcium ion loose water molecules from its hydration sphere inside the pores of the resin. The proton self-diffusion coefficient in a phenol sulfonic - formaldehyde resin type gel was of $2.4 \cdot 10^{-9}$ $m^2 s^{-1}$ [21, 22]. The proton self-diffusion coefficient evaluated in this work for the sulfonated macronet resin is of $3 \cdot 10^{-10}$ $m^2 s^{-1}$. The evaluated coefficient is around ten times smaller in the sulfonated hyper-reticulated resin, than in phenolsulfonic-formaldehyde type gel resin and 30 times smaller than in dilute aqueous solution. This behavior supports the hypotheses that the sulfonic groups in the macronet resin are distributed also in micropores, not only in the macropores, as it is the popular image for the macroporous resins. The quasi-homogeneous resin phase hypothesis is a rough one for the macronet resin having macro-, meso- and micropores.

The experimental kinetic data were also modeled with a bidisperse pore proposed model [14]. The macro- and mesopores are considered "macropores" and thus the MN500 resin can be considered as having a bidisperse pore structure. Three hypotheses were analyzed. A) The ion interdiffusion was considered thousand times faster in macropores than in micropores, thus the ion exchange

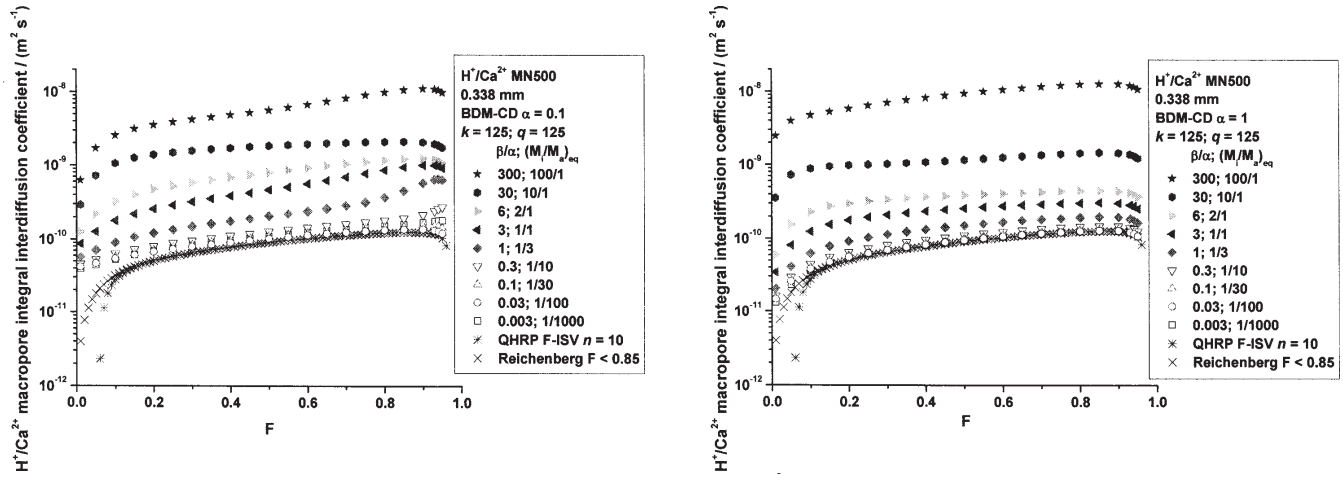

Fig. 7. H^+/Ca^{2+} macropore integral interdiffusion coefficients on macronet MN500 resin obtained with BDM-CD kinetic model; 298 K; 0.95 eq/L $Ca(NO_3)_2$

α	β/α	$\overline{D}_{F=0.01}\cdot10^{10}$ ($m^2\ s^{-1}$)	$\overline{D}_{F=0.5}\cdot10^{10}$ ($m^2\ s^{-1}$)	$\overline{D}_{max}\cdot10^{10}$ ($m^2\ s^{-1}$)
0.001	0.003		1.19	1.53
0.001	0.03		1.21	1.59
0.001	0.05		1.23	1.64
0.001	0.1		1.28	21.4*
0.001	0.3		1.50	76.6*
0.001	1		2.52	89.8*
0.001	3		14.5	579*
0.001	6		290*	579*
0.001	30		579*	579*
0.001	300		579*	579*
0.1	0.03	0.357	1.34	1.68
0.1	0.05	0.357	1.34	1.68
0.1	0.1	0.367	1.42	1.85
0.1	0.3	0.394	1.67	3.60
0.1	1	0.491	2.69	7.84
0.1	3	0.744	6.05	12.1
0.1	6	1.07	10.4*	15.0*
0.1	30	2.52	24.0*	26.0*
0.1	300	5.34	73.8*	134*
1	0.003	0.111	1.20	1.54
1	0.03	0.125	1.23	1.56
1	0.05	0.126	1.25	1.58
1	0.1	0.128	1.29	1.63
1	0.3	0.138	1.44	1.81
1	1	0.174	1.97	2.39
1	3	0.294	3.35	3.75
1	6	0.514	5.04	5.44
1	30	3.04	15.1*	17.8*
1	300	21.9*	123*	156*

*meaningless

Table 8
H^+/Mg^{2+} MACROPORE INTEGRAL INTERDIFFUSION COEFFICIENTS ON THE STRONG ACID MACRONET RESIN MN500 OBTAINED WITH BDM KINETIC MODEL FOR DIFFERENT VALUES OF α AND β/α PARAMETERS

being a step-by-step process [14]. The macropore interdiffusion coefficients were obtained with equation 7 (BDM-LC) using a computer program previously reported [7, 8, 16, 17, 23, 24] for different values of the unknown β/α parameter and the results are given in figure 6 for both systems. B) The ion interdiffusion was considered to be competitive in macro- and micropores, but ten times faster in macropores than in micropores. The macropore interdiffusion coefficients for different values of β/α parameters and α = 0.1 were computed with equation 6 using a computer programs reported in previous papers [7, 8, 24], and the results are given in figures 6 and 7 for H^+/Mg^{2+} and H^+/Ca^{2+} on sulfonated macronet resin, respectively. C) The last case assumed a competitive diffusion in macro-and micropores with the same rate. The macropore interdiffusion coefficients were computed with equation 6 for α = 1 and different values of β/α parameter, and the results are given in figures 5 and 6 for the two investigated systems.

The macropores integral interdiffusion coefficients at F = 0.01, 0.5 and the maximum value obtained with BDM for α = 0.001, 0.1 and 1 and different β/α parameters are given in table 8 for H^+/Mg^{2+} and in table 9 for H^+/Ca^{2+} on the sulfonated macronet resin. It must be noted that equation 7 is not convergent for n = 10, thus the interdiffusion coefficients for: α = 0.001 and F = 0.01 were not given.

The obtained coefficients were compared with the proton self-diffusion coefficient in dilute aqueous solution

Table 9

H^+/Ca^{2+} MACROPORE INTEGRAL INTERDIFFUSION COEFFICIENTS ON THE STRONG ACID MACRONET RESIN MN500 OBTAINED WITH BDM KINETIC MODEL FOR DIFFERENT VALUES OF α AND β/α PARAMETERS

α	β/α	$\overline{D}_{F=0.01}\cdot10^{10}$ ($m^2\ s^{-1}$)	$\overline{D}_{F=0.5}\cdot10^{10}$ ($m^2\ s^{-1}$)	$\overline{D}_{max}\cdot10^{10}$ ($m^2\ s^{-1}$)
0.001	0.003		0.919	1.28
0.001	0.01		0.924	1.29
0.001	0.03		0.940	1.33
0.001	0.05		0.955	1.37
0.001	0.075		0.975	1.44
0.001	0.1		0.995	1.52
0.001	0.3		1.17	123*
0.001	1		1.95	478*
0.001	3		11.2*	578*
0.01	0.003	0.391	1.11	1.84
0.01	0.03	0.418	1.04	1.40
0.01	0.1	0.429	1.10	1.56
0.01	0.3	0.460	1.30	2.79
0.01	1	0.574	2.08	6.63
0.01	3	0.870	4.69	10.2
0.01	6	1.26	8.05	12.6
0.01	30	2.94	18.6*	21.4*
0.01	300	6.25	57.1*	113*
1	0.003	0.130	0.934	1.28
1	0.03	0.146	0.956	1.30
1	0.1	0.150	0.996	1.36
1	0.3	0.161	1.11	1.50
1	1	0.204	1.52	1.99
1	3	0.343	2.60	3.10
1	6	0.600	3.90	4.49
1	30	3.56	11.7	14.8
1	300	24.8*	95.0*	130*

*meaningless

Table 10

UPPER LIMIT OF β/α PARAMETERS FOR A GIVEN α FOR H^+/Mg^{2+} AND H^+/Ca^{2+} INTERDIFFUSION INSIDE THE STRONG ACID MACRONET RESIN MN500; 0.338 mm; 298 K

Model	α	β/α	$M_{i\infty}/M_{a\infty}$	$\overline{D}_{F=0.01}\cdot10^{10}$ ($m^2\ s^{-1}$)	$\overline{D}_{F=0.5}\cdot10^{10}$ ($m^2\ s^{-1}$)	$\overline{D}_{max}\cdot10^{10}$ ($m^2\ s^{-1}$)
				H^+/Mg^{2+}		
BDM-LC	0.001	0.1	1/30		1.28	21.4
BDM-CD	0.1	6	2/1	1.07	10.4	15.0
BDM-CD	1	30	10/1	3.04	15.1	17.8
Paterson				0.0305	1.18	3.25
$t_{1/2}\ vs.\ \bar{r}_0^2$					1.23	
				H^+/Ca^{2+}		
BDM-LC	0.001	0.1	1/30		0.995	1.52
BDM-CD	0.1	6	2/1	1.26	8.05	12.6
BDM-CD	1	30	10/1	3.56	11.7	14.8
Paterson				0.031	0.97	2.98
$t_{1/2}\ vs.\ \bar{r}_0^2$					1.01	

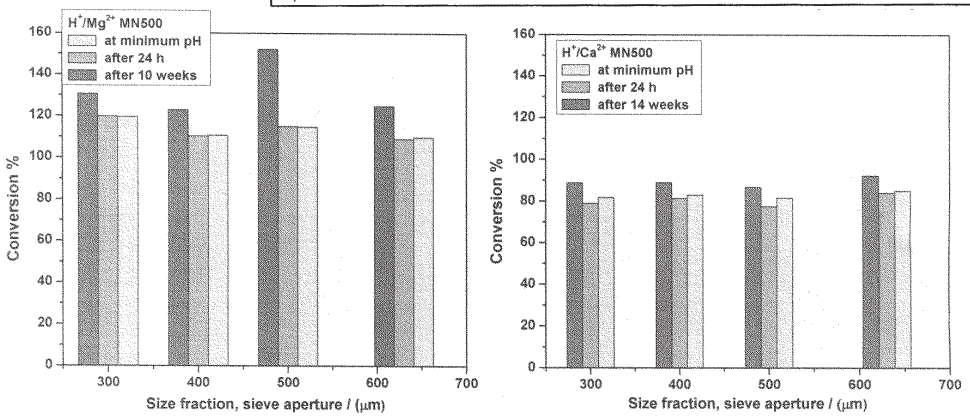

Fig. 8. Conversion for H^+/Mg^{2+} and H^+/Ca^{2+} ion exchange processes on strong acid macronet MN500 resin; 298 K; 0.93 eq/L $Mg(NO_3)2$; 0.95 eq/L $Ca(NO_3)_2$

and with the interdiffusion coefficients obtained with QHRP models. The interdiffusion coefficients higher than the value for proton in dilute aqueous solution were disregarded being meaningless together with the corresponding β/α parameters. The upper limit of β/α was evaluated for each α, and the results are collected in table 10 for both investigated systems. Taking into account the correspondence between β/α and the ratio of the uptake

at equilibrium in micropores and macropores (table1), the upper limit of the ratio between the sulfonic acid groups bound in micropores and macropores was revealed. The hypothesis of a step-by-step diffusion in macropores and in micropores lead to the conclusion that to one functional group bound in micropores at least 30 groups are bound in macropores. The assumption of a competitive diffusion in macropores and micropores ten times faster in macropores showed that the ratio between the number of sulfonic groups existing in micropores and macropores should be less than two. The last hypothesis was competitive diffusion in macro- and micropores with the same rate, and the results showed that the ratio between the number of the sulfonic groups bound in micropores and macropores should be less than ten.

Figure 8 gives a comparison between the conversion of the resin for H^+/Mg^{2+} and H^+/Ca^{2+} ion exchange processes on sulfonated macronet ion exchanger. The conversion was calculated as the ratio between the loading and the ion exchange capacity of the resin (table 2). It must be noted that a minimum value of the *p*H was reached in the kinetic run, and after this moment the *p*H increased slightly, probably due to hydrolysis of the resinate. After a long time (10-14 weeks) the metal ion exchanged a larger amount of functional groups, and the conversion increased for all size fractions, showing a very slow rate of ion exchange near equilibrium. It must be noted that for H^+/Ca^{2+} the hydrolysis was of 1-2 % for different size fractions, but for H^+/Mg^{2+} the hydrolysis was negligible. The ion exchanger MN500 accepted a larger amount of magnesium ion than the ion exchange capacity determined by the standard method even at short time, which could be explained by electrolyte sorption favoured by a strong interaction cation-π-electrons of the aromatic rings of the matrix. Calcium ion has a larger radius and cannot penetrate in small pores, and creates a weaker electric field than magnesium ion.

Conclusions

The H^+/Mg^{2+} and H^+/Ca^{2+} ion exchange kinetics on a relatively new polystyrenic resin with sulfonic functional groups and a hypercrosslinked matrix Purolite MN500, were investigated in order to evaluate this material in the demineralization process. This ion exchanger has macro-, meso- and micropores. The ion exchange rate was measured at 298 K using a potentiometric method in conditions favoring a mechanism controlled by particle diffusion. The interdiffusion coefficients were obtained with quasi-homogeneous resin phase kinetic models (QHRP) and with a bidisperse pore kinetic model (BDM). It was shown that QHRP models at infinite solution volume gives results for interdiffusion coefficients in good agreement with QHRP at finite solution volume for kinetic experiments done in a batch reactor when the ratio between the solution volume and the mass of the resin was 100 mL/g, and the amount of the ion in the resin phase and in the solution phase was less than 0.03. The BDM allowed the calculation of the macropore interdiffusion coefficients in three different hypotheses: A) a step-by-step- interdiffusion in macropores and micropores; B) a competitive inter-diffusion in macropores and micropores but ten times faster in macropores; C) a competitive interdiffusion in macro- and micropores with equal rates. The evaluated upper limit of the ratio between the functional groups bound in micropores and macropores of the macronet resin were 1/30, 2/1, 10/1 if we assume the hypotheses A), B), and C), respectively. The macronet matrix produced a notable retarding effect on proton/magnesium(II) and proton/calcium(II) ion exchange due to interdiffusion also in micropores. The self-diffuion coefficients of proton, magnesium(II) and calcium(II) in the macronet resin were evaluated.

Acknowledgements: The authors acknowledge Purolite International Ltd. for supplying the resin.

List of symbols

$\overline{D}$ - effective intraparticle diffusivity; self-diffusion coefficient for isotopic exchange; integral interdiffusion coefficient for mutual ion-exchange ($m^2\ s^{-1}$)

$\overline{D}_a$ - effective macropore diffusivity; macropore self-diffusion coefficient for isotopic exchange; macropore integral interdiffusion coefficient for mutual ion-exchange ($m^2\ s^{-1}$)

D_i - effective micropore diffusivity; micropore self-diffusion coefficient for isotopic exchange; micropore integral interdiffusion coefficient for mutual ion-exchange ($m^2\ s^{-1}$)

number of ion equivalents at equilibrium in the resin and solution e, $\overline{e}$, e - phases (eq)

F - fractional attainment of equilibrium (dimensionless)

$M_{a\infty}$ - macropore uptake at equilibrium (eq/kg)

$M_{i\infty}$- micropore uptake at equilibrium (eq/kg)

n - number of terms in a series

pH_o pH_∞ pH_i - pH of the external solution at start, equilibrium and time *t*

$\overline{r}_o$ - average radius of the resin swollen beads (m)

r_i - microsphere radius (m)

S_n - roots of equation $S_n\ cot\ S_n = 1 + S_n^2/3w$

t - time (s)

$t_{1/2}$ - Half-time (s)

Greek symbols

$\alpha = \overline{D}_i \overline{r}_0^2 / \overline{D}_a \overline{r}_i^2$ = dimensionless rate parameter

$\beta / \alpha = 3 M_{i\infty} / M_{a\infty}$ - dimensionless equilibrium parameter

α', β' - roots of equation $x^2+3\omega x - 3\omega = 0$

$\theta = \overline{D}_a t / \overline{r}_0^2$ - dimensionless time

$\tau = \overline{D} t / \overline{r}_0^2$ - dimensionless time

$\omega = \overline{e} / e$ - dimensionless equilibrium parameter

References

1.The Purolite Company, Purolite Technical Bulletin, Hypersol-Macronet Sorbent Resins, The Purolite Company, Bala Cynwyd, PA, 1999

2.JORGENSEN, T.C., WEATHERLEY, L.R., Water Res., **37**, 2003, p 1723

3.BOHDANA, C.M., CANTEA, D.S., PINCOVSCHI, E., OANCEA, A.M.S., Rev. Chim. (Bucharest), **62**, no.2, 2011, p 233

4.BOHDANA, C.M., PINCOVSCHI, E., OANCEA, A.M.S., Rev. Chim. (Bucharest), **63**, no.2, 2012, p 159

5.OANCEA, A.M.S., DRINKAL, C., HÖLL, W.H., J. Ion Exchange (Japan), **18**, nr. 4, 2007, p.162

6.OANCEA, A.M.S., DRINKAL, C., HÖLL, W.H., React. Funct. Polym., **68**, (2008), p 492

7.OANCEA, A.M.S., RADULESCU, M., OANCEA, D., PINCOVSCHI, E., Ind. Eng.. Chem. Res. **45**, 2006, p. 9096

8.OANCEA, A.M.S., POPESCU, A.R., RADULESCU, M., WEBER, V., PINCOVSCHI, E., COX, M., Solvent Extr. Ion Exch., **26**, 2008, p. 217

9.TSYURUPA, M.P., DAVANKOV, V.A., React. Funct. Polym., **53**, 2002, p 193

10.TSYURUPA, M.P., DAVANKOV, V.A., React. Funct. Polym., **66**, 2006, p 768

11.BOHDANA, C.M., CANTEA, D.S., DALE, J.A., PINCOVSCHI, E., OANCEA, A.M.S. , Recent Advences in Ion Exchange Theory & Practice, Proceedings of IEX2008, Editor M. Cox, SCI, Cambridge, 2008, p. 427

12.HELFFERICH, F., Ion Exchange **1995**, Dover Publications, Inc., New York, chapter 6, p 250
13.REICHENBERG, D., J. Am. Chem. Soc. **75**, 1953, p. 589.
14.RUCKENSTEIN, E., VAIDYANATHAN, A.S., YOUNGQUIST, G.R, Chem. Eng. Sci., **26**, 1971, p. 1305
15.ZUYI, T., AIMIN, Z., WENGONG, T., RONG, X., XINGQU, C., Zuyi, T.; J. Radioanal. Nucl. Chem., **116**, 1987, p. 35
16.OANCEA, A.M.S., PINCOVSCHI, E., OANCEA, D., COX, M., Hydrometallurgy **62**, 2001, p. 31
17.OANCEA, A.M.S., RADULESCU, M., PINCOVSCHI, E., COX, M., OANCEA, Solvent. Extr. Ion. Exch. **23**, 2005, p. 131
18NIGHTINGALE, E.R. Jr., J. Phys. Chem, **63**, 1959, p. 1381
19 HUEEY, J.E., KEITER, E.A., KEITER R.L., Chimie Inorganique, De Boeck & Larcier s.a., 1996, Paris, p. 114
20.LINDE, D.R., EDITOR, CRC HANDBOOK OF CHEMISTRY AND PHYSICS, 85th edition 2005, CRC Press, Boca Raton, 2005; Section 5, table 5-93
21.HELFFERICH, F., J. Phys. Chem. **66**, 1962, p. 39
22.HELFFERICH, F., J. Phys. Chem. **67**, 1963, p. 1157
23.WEBER, V., POPESCU, A.R., OANCEA, A.M.S., Rev. Chim. (Bucharest), **59**, no.5, 2008, p 519
24.RADULESCU, M., COX, M., OANCEA, A.M.S., Solvent Extr. Ion. Exch. **30**, 2012, p. 372

Manuscript received: 4.10.2012